

UVO Challenge on Video-based Open-World Segmentation 2021: 1st Place Solution

Yuming Du¹

Wen Guo²

Yang Xiao¹

Vincent Lepetit¹

¹LIGM, Ecole des Ponts, Univ Gustave Eiffel, CNRS, Marne-la-Vallée, France

²Inria, Univ. Grenoble Alpes, CNRS, Grenoble INP, LJK, 38000 Grenoble, France

{yuming.du, yang.xiao, vincent.lepetit}@enpc.fr, wen.guo@inria.fr

https://github.com/dulucas/UVO_Challenge

Abstract

In this report, we introduce our (pretty straightforward) two-step “detect-then-match” video instance segmentation method. The first step performs instance segmentation for each frame to get a large number of instance mask proposals. The second step is to do inter-frame instance mask matching with the help of optical flow. We demonstrate that with high quality mask proposals, a simple matching mechanism is good enough for tracking. Our approach achieves the first place in the UVO 2021 Video-based Open-World Segmentation Challenge.

1. Method

In this section, we present our detect-then-matching method for open-world video instance segmentation. Our method consists of two steps, the first step is to generate mask proposals for each frame of the video. The second step aims to link the detected masks using optical flow predicted by an optical flow estimator.

1.1. First Step: Instance Segmentation

In this section, we introduce our method for instance segmentation. We adopt a detect-then-segment pipeline. We first train an object detector to generate bounding boxes for each frame of the video. Then, we take the top-100 bounding box proposals, crop the images with these bounding boxes and feed the resized obtained image patches to a foreground/background segmentation network to obtain instance masks. We briefly introduce the networks that we used for instance segmentation, please refer to our technical report for Image-based open-world segmentation for more details[6].

Detection Network. We adopt the Cascade Region Proposal Network (RPN) [20] as our baseline network, and the

Focal loss [12] and GIoU loss [17] for classification and bounding box regression. We use two separate SimOTA [8] samplers for positive/negative example sampling during training, with one for classification and another for bounding box regression. We loose the selection criterion for bounding box regression sampler to get more positive samples for the bounding box head during training. An additional IoU branch is added in parallel with classification head and bounding box regression head to predict the IoU between the predicted bounding box and the ground truth bounding box. Following previous works [8, 19], we adopt the decoupled head to ease the conflict between classification task and regression task in object detection. Heads across all pyramid levels share the same weights to save memory. The first convolutional layer of the decoupled heads is replaced by deformable convolutional layers [4]. We add CARAFE [21] blocks in our FPN [11] and use Swin-L transformer [14] as our backbone network.

Segmentation We use the bounding boxes predicted by our detection network to crop image patches and resize them to 512×512 . The cropped image patches are then fed to our segmentation network to get instance masks. We adopt the Upernet [23] architecture and Swin-L transformer [14] as our backbone for segmentation network. The segmentation network is a binary segmentation network, the pixels are predicted as foreground if they belong to an object, otherwise as background.

1.2. Second Step: Mask Matching across Frames

In this section, we introduce our matching method for video instance segmentation. An overview of our method is shown in Figure 1. Our idea is similar to IoU-tracker. The trackers from previous frame are wrapped to current frame using predicted optical flow, then the trackers are matched with detected mask proposals from current frame by calculating the IoU (Intersection-over-Union) between

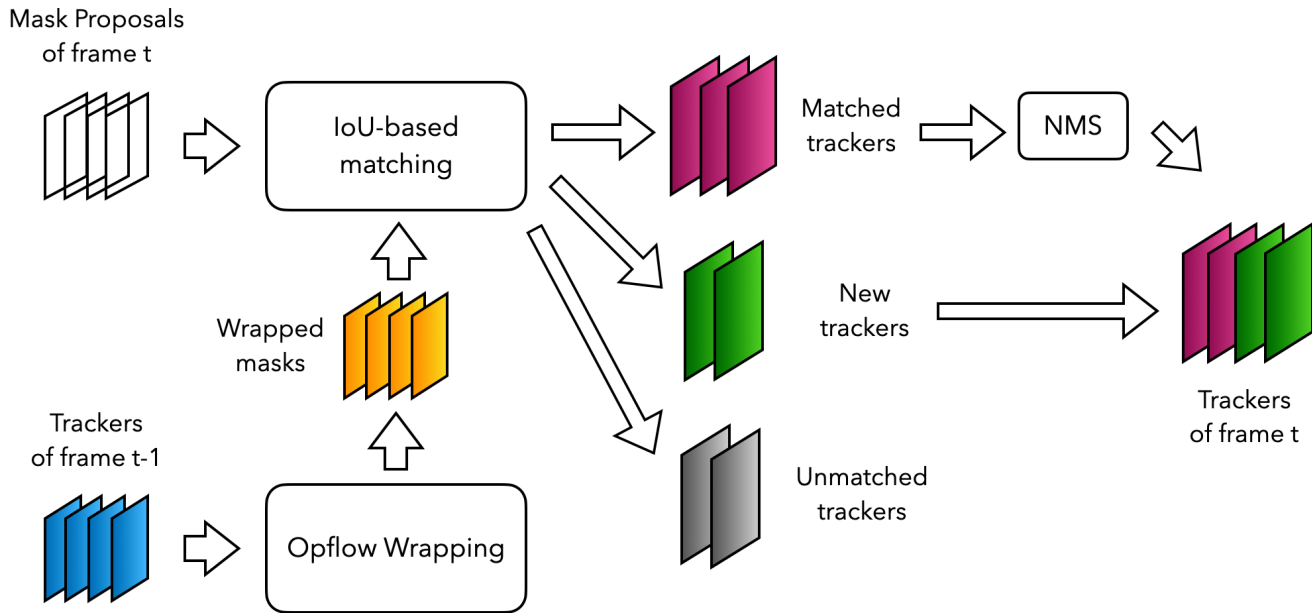


Figure 1. **Overview of our mask matching pipeline.** The masks of the different trackers from frame $t - 1$ are first wrapped using optical flow F_{t-1} , then we match the wrapped masks with detected masks from frame t . The trackers that do not have any matched masks will be removed if they stay without matches for 5 frames. The matched tracker will update their latest mask to their matched masks. The unmatched detected masks are used to initialize new trackers and will be added to the total trackers.

the wrapped masks of trackers and the detected masks.

We denote M as the total mask proposals for all frames, with M_t represents the mask proposals for frame t . T denotes the video length and F denotes the optical flows where F_t represent the optical flow between frame t and frame $t + 1$.

We first initialize trackers with the mask proposals from the first frame M_0 . Then, we wrap the masks of the trackers to the second frame using optical flow F_0 . The wrapped masks are then matched with the detected masks M_1 by calculating the IoU between them. We consider a matching is successful only if the IoU is larger than a fixed threshold, which is 0.5 in our case. If a tracker is matched with a detected mask, we replace the latest mask of the tracker with the matched mask. If there is no match between the tracker and the masks from M_1 , the wrapped mask is used to update its latest mask. If the tracker has not been matched continuously for 5 frames, we remove this tracker from our tracker list. For the masks from M_1 that are not been matched with trackers, we initialize new trackers with these masks and add these trackers to our tracker list. We use NMS (Non-maximum-suppression) to remove the trackers whose latest masks have an IoU larger than 0.7.

We assign each tracker with a score, which is calculated as the product between the number of frames that it has been tracked and the sum of the detection scores.

2. Dataset

2.1. Detection

ImageNet 22k is used to pre-train our backbone network. We then train our detectors on the COCO dataset [13]. In the end, the pre-trained detectors are fine-tuned on UVO-Sparse dataset and UVO-Dense dataset [22].

2.2. Segmentation

ImageNet 22k [5] is used to pre-train our backbone network. We then train our segmentation network on a combination of the OpenImage [10], PASCALVOC [7], and COCO [13] datasets. In the end, the pre-trained segmentation networks are fine-tuned on the UVO-Sparse and UVO-Dense datasets [22].

3. Implementation Details

3.1. Detection

We use MMDetection [2] to train our detectors. For the backbone network, we get the Swin-L transformer pre-trained on ImageNet 22k from ¹. All our detectors are trained with Detectron ‘1x’ setting. For data augmentation, we use the basic data augmentation strategy as in [9] for all experiments. The center ratio of both SimOTA samplers are set to 0.25, the top-K number for classification head is set

¹<https://github.com/microsoft/Swin-Transformer>

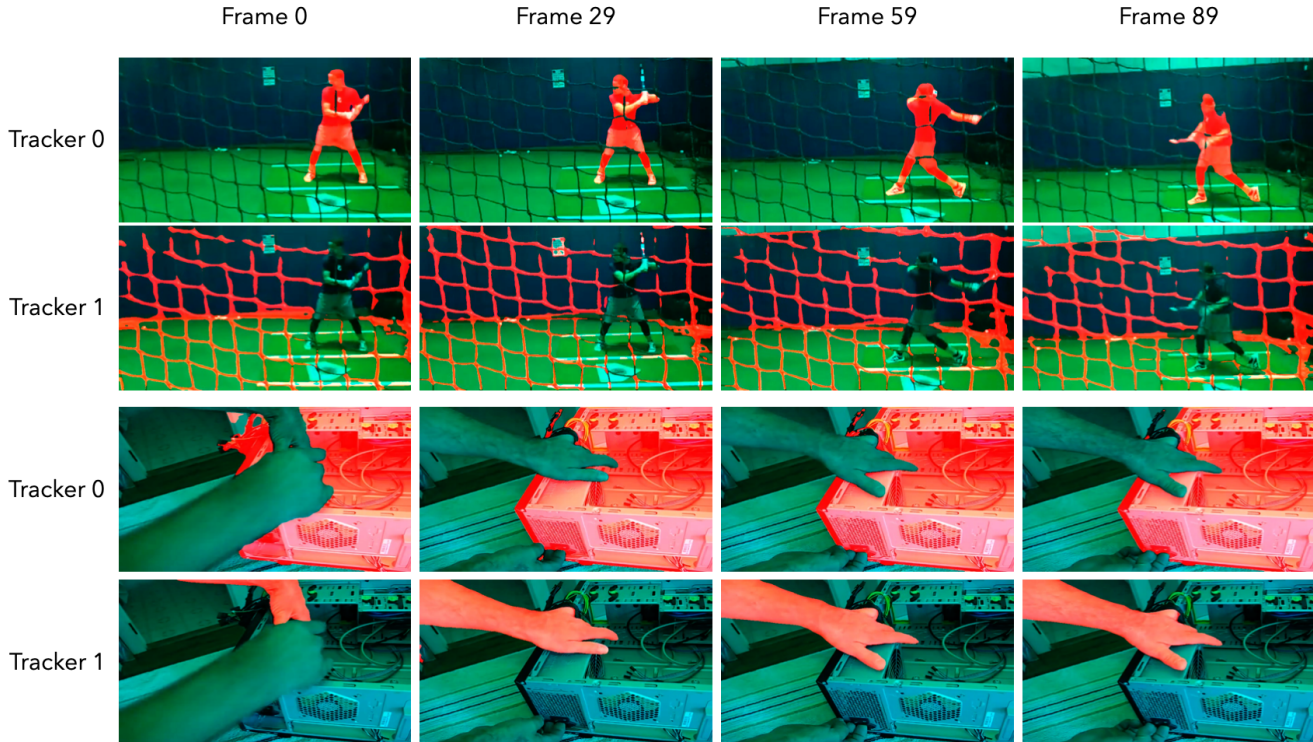


Figure 2. Examples of results of our video instance segmentation approach on the UVO-Dense test dataset.

to 10, while the top-K number for regression head is set to 20 to involve more positive samples. Four 3x3 conv layers are used in the classification branch and the regression head, IoU branch shares the same conv layers with the regression branch. To train the detector with Swin-L transformer backbone, we adopt the AdamW as the optimizer and set the init learning rate to $1e-4$. The batch size is set to 16. After training on COCO, we fine-tune the detector on the combination of the UVO-Sparse and UVO-Dense datasets for 6 epochs. All our detectors are trained in the class-agnostic way. Test time augmentation is used during inference to further boost the network performance.

3.2. Segmentation

We use MMSegmentation [3] to train our segmentation network. We use the same backbone network as our detection network. During training, given an image and an instance mask, we first generate a bounding box that envelopes the instance mask, then a 20 pixel margin is added to the bounding box in all directions. We use the generated bounding box to crop the image and resize the image patch to 512x512. Random flipping, random photometric distortion, and random bounding box jitter are used as data augmentation. We adopt 'poly' learning rate policy and set the initial learning rate to $6e-5$. The batch size is set to 32 and AdamW [15] is used as the optimizer. We first train

our network on the combination of the OpenImage [10], PASCALVOC [7] and COCO [13] datasets for 300k iterations, then we finetune the network on the combination of the UVO-Dense and UVO-Sparse datasets for 100k iterations with initial learning rate set to $6e-6$. All our segmentation networks are trained in a class-agnostic way, thus, segmenting the object in the cropped path becomes a foreground/background segmentation problem. Only flip test augmentation was used during inference.

3.3. Optical Flow Estimation

We use the model released by [18] trained on FlyingThings [16]. FlyingThings is a large-scale synthetic dataset for optical flow estimation. The dataset is generated by randomizing the movement of the camera and synthetic objects collected from the ShapeNet dataset [1]. The model for optical flow estimation is pre-trained on FlyingThings for 100k iterations with a batch size of 12, then for 100k iterations on FlyingThings3D with a batch size of 6.

4. Visualization

In Figure 2, we show some of our the video instance segmentation results. Our method works well for objects of different shapes.

Teams	AR@100	AP	AP@.5	AP@.75	AR@1	AR@10
Baseline by host	11.77	7.35	16.33	6.10	5.06	11.72
CSTT(lvis_htc_4_s0.002)	26.98	16.96	31.16	15.22	6.99	22.04
Sensetime	29.04	18.16	32.09	17.46	7.22	24.14
elf_hzw (final)	34.00	14.13	23.50	14.52	7.45	21.14
Ours	41.17	27.56	40.61	29.22	8.96	29.92

Table 1. **Challenge final results** on UVO-Sparse test dataset. Our method outperforms the baseline and the other submitted methods by a large margin.

5. Potential Improvements

Our simple “detect-then-match” framework can serve as a baseline for video instance segmentation. It heavily relies on the quality of mask proposals for each frame. The performance of our method could be affected by heavy occlusion, object appearance/disappearance/re-appearance, etc. These problems could be potentially solved by taking object embedding into consideration during the mask matching process.

References

- [1] Angel X. Chang, Thomas Funkhouser, Leonidas Guibas, Pat Hanrahan, Qixing Huang, Zimo Li, Silvio Savarese, Manolis Savva, Shuran Song, Hao Su, Jianxiong Xiao, Li Yi, and Fisher Yu. ShapeNet: An Information-Rich 3D Model Repository. Technical Report arXiv:1512.03012 [cs.GR], Stanford University — Princeton University — Toyota Technological Institute at Chicago, 2015.
- [2] Kai Chen, Jiaqi Wang, Jiangmiao Pang, Yuhang Cao, Yu Xiong, Xiaoxiao Li, Shuyang Sun, Wansen Feng, Ziwei Liu, Jiarui Xu, Zheng Zhang, Dazhi Cheng, Chenchen Zhu, Tianheng Cheng, Qijie Zhao, Buyu Li, Xin Lu, Rui Zhu, Yue Wu, Jifeng Dai, Jingdong Wang, Jianping Shi, Wanli Ouyang, Chen Change Loy, and Dahua Lin. MMDetection: Open mmlab detection toolbox and benchmark. *arXiv preprint arXiv:1906.07155*, 2019.
- [3] MMSegmentation Contributors. MMSegmentation: Openmmlab semantic segmentation toolbox and benchmark. <https://github.com/open-mmlab/mms Segmentation>, 2020.
- [4] Jifeng Dai, Haozhi Qi, Yuwen Xiong, Yi Li, Guodong Zhang, Han Hu, and Yichen Wei. Deformable convolutional networks. In *Proceedings of the IEEE international conference on computer vision*, pages 764–773, 2017.
- [5] J. Deng, W. Dong, R. Socher, L.-J. Li, K. Li, and L. Fei-Fei. ImageNet: A Large-Scale Hierarchical Image Database. In *CVPR09*, 2009.
- [6] Yuming Du, Wen Guo, Yang Xiao, and Vincent Lepetit. 1st place solution for the uvo challenge on image-based open-world segmentation 2021. *arXiv preprint arXiv:2110.10239*, 2021.
- [7] Mark Everingham, Luc Van Gool, Christopher KI Williams, John Winn, and Andrew Zisserman. The pascal visual object classes (voc) challenge. *International journal of computer vision*, 88(2):303–338, 2010.
- [8] Zheng Ge, Songtao Liu, Feng Wang, Zeming Li, and Jian Sun. Yolox: Exceeding yolo series in 2021. *arXiv preprint arXiv:2107.08430*, 2021.
- [9] Kaiming He, Georgia Gkioxari, Piotr Dollár, and Ross Girshick. Mask r-cnn. In *Proceedings of the IEEE international conference on computer vision*, pages 2961–2969, 2017.
- [10] Ivan Krasin, Tom Duerig, Neil Alldrin, Vittorio Ferrari, Sami Abu-El-Haija, Alina Kuznetsova, Hassan Rom, Jasper Uijlings, Stefan Popov, Shahab Kamali, Matteo Mallocci, Jordi Pont-Tuset, Andreas Veit, Serge Belongie, Victor Gomes, Abhinav Gupta, Chen Sun, Gal Chechik, David Cai, Zheyun Feng, Dhyanes Narayanan, and Kevin Murphy. Openimages: A public dataset for large-scale multi-label and multi-class image classification. *Dataset available from https://storage.googleapis.com/openimages/web/index.html*, 2017.
- [11] Tsung-Yi Lin, Piotr Dollár, Ross Girshick, Kaiming He, Bharath Hariharan, and Serge Belongie. Feature pyramid networks for object detection. In *Proceedings of the IEEE conference on computer vision and pattern recognition*, pages 2117–2125, 2017.
- [12] Tsung-Yi Lin, Priya Goyal, Ross Girshick, Kaiming He, and Piotr Dollár. Focal loss for dense object detection. In *Proceedings of the IEEE international conference on computer vision*, pages 2980–2988, 2017.
- [13] Tsung-Yi Lin, Michael Maire, Serge Belongie, James Hays, Pietro Perona, Deva Ramanan, Piotr Dollár, and C Lawrence Zitnick. Microsoft coco: Common objects in context. In *European conference on computer vision*, pages 740–755. Springer, 2014.
- [14] Ze Liu, Yutong Lin, Yue Cao, Han Hu, Yixuan Wei, Zheng Zhang, Stephen Lin, and Baining Guo. Swin transformer: Hierarchical vision transformer using shifted windows. *arXiv preprint arXiv:2103.14030*, 2021.
- [15] Ilya Loshchilov and Frank Hutter. Decoupled weight decay regularization. *arXiv preprint arXiv:1711.05101*, 2017.
- [16] N. Mayer, E. Ilg, P. Häusser, P. Fischer, D. Cremers, A. Dosovitskiy, and T. Brox. A large dataset to train convolutional networks for disparity, optical flow, and scene flow estimation. In *IEEE International Conference on Computer Vision and Pattern Recognition (CVPR)*, 2016. arXiv:1512.02134.

- [17] Hamid Rezatofghi, Nathan Tsoi, JunYoung Gwak, Amir Sadeghian, Ian Reid, and Silvio Savarese. Generalized intersection over union: A metric and a loss for bounding box regression. In *Proceedings of the IEEE/CVF Conference on Computer Vision and Pattern Recognition*, pages 658–666, 2019.
- [18] Zachary Teed and Jia Deng. Raft: Recurrent all-pairs field transforms for optical flow. In *European conference on computer vision*, pages 402–419. Springer, 2020.
- [19] Zhi Tian, Chunhua Shen, Hao Chen, and Tong He. Fcos: Fully convolutional one-stage object detection. In *Proceedings of the IEEE/CVF international conference on computer vision*, pages 9627–9636, 2019.
- [20] Thang Vu, Hyunjun Jang, Trung X Pham, and Chang D Yoo. Cascade rpn: Delving into high-quality region proposal network with adaptive convolution. *arXiv preprint arXiv:1909.06720*, 2019.
- [21] Jiaqi Wang, Kai Chen, Rui Xu, Ziwei Liu, Chen Change Loy, and Dahua Lin. Carafe: Content-aware reassembly of features. In *Proceedings of the IEEE/CVF International Conference on Computer Vision*, pages 3007–3016, 2019.
- [22] Weiyao Wang, Matt Feiszli, Heng Wang, and Du Tran. Unidentified video objects: A benchmark for dense, open-world segmentation. *arXiv preprint arXiv:2104.04691*, 2021.
- [23] Tete Xiao, Yingcheng Liu, Bolei Zhou, Yuning Jiang, and Jian Sun. Unified perceptual parsing for scene understanding. In *Proceedings of the European Conference on Computer Vision (ECCV)*, pages 418–434, 2018.